Hindawi Publishing Corporation
International Journal of Photoenergy
Volume 2015, Article ID 592079, 6 pages
http://dx.doi.org/10.1155/2015/592079

Research Article

Influence of Secondary Phases in Kesterite-Cu_2ZnSnS_4 Absorber Material Based on the First Principles Calculation

Wujisiguleng Bao and Masaya Ichimura

Department of Engineering Physics, Electronics and Mechanics, Nagoya Institute of Technology, Gokiso, Showa-ku, Nagoya 466-8555, Japan

Correspondence should be addressed to Masaya Ichimura; ichimura.masaya@nitech.ac.jp

Received 7 March 2014; Revised 22 July 2014; Accepted 8 September 2014

Academic Editor: Cooper H. Langford

The influence of secondary phases of ZnS and Cu_2SnS_3 (CTS) in Cu_2ZnSnS_4 (CZTS) absorber material has been studied by calculating the band offsets at the CTS/CZTS/ZnS multilayer heterojunction interfaces on the basis of the first principles band structure calculation. The ZnS/CZTS heterointerface is of type I and since ZnS has a larger band gap than that of CZTS, the ZnS phase in CZTS is predicted to be resistive barriers for carriers. The CTS/CZTS heterointerface is of type I; that is, the band gap of CTS is located within the band gap of CZTS. Therefore, the CTS phase will act as a recombination site in CZTS.

1. Introduction

As candidates for low-cost and nontoxic thin-film solar-cell absorbers, quaternary semiconductor Cu_2ZnSnS_4 (CZTS) has attracted much attention recently as an absorber layer material in a heterojunction solar cell [1–6]. It is a direct-band gap p-type semiconductor having a 1.5 eV band gap, which is close to the optimum band gap for solar cells [7–9].

Because of the increased number of elements in CZTS, their synthesis is more difficult than for binary and ternary semiconductors. The secondary phases in CZTS, such as ZnS, Cu_2S, and Cu_2SnS_3 (CTS), could form depending on the processing conditions [10–12]. Experimentally it is found that working devices are obtained for "Cu-poor" and "Zn-rich" compositions [13]. It has been theoretically shown that ZnS and CTS have relatively small formation enthalpies among the above secondary phases [14].

Presence of the secondary phases could affect the photovoltaic performance. It has been speculated that the phase separation of CZTS into ZnS and Cu-Sn-S compounds is one of the factors limiting the efficiency of CZTS solar cells [12, 15–19]. However, the effects of the secondary phases on solar cell performance can in fact be significantly different depending on the band offset with CZTS. There are several possible band alignments at heterointerfaces between CZTS and secondary phases as shown in Figure 1. If the band alignment is of type I, the conduction band minimum (CBM) of the secondary phase is higher (or lower) than that of CZTS, and the valence band maximum (VBM) of the secondary phase is lower (or higher) than that of CZTS, as shown in Figures 1(a) and 1(b), depending on whether the band gap of the secondary phase is larger or smaller than that of CZTS. If the band gap is smaller, the secondary phase will act as a sink for both the minority and majority carriers and facilitate the carrier recombination. Thus the carrier separation is hampered, and the carrier collection efficiency of the cell would be reduced. When the secondary phase has a larger band gap (Figure 1(b)), the band offset should become a barrier for both of the minority and majority carriers in CZTS. Then, the secondary phase just reduces the conductivity but does not enhance carrier recombination rate in the absorber layer. On the other hand, if the band alignment is of type II, both of CBM and VBM for the secondary phase are lower or higher than that of CZTS, as shown as Figures 1(c) and 1(d). In those cases, the secondary phase acts as a sink for only one type of carrier; that is, electrons and holes tend to be separated, and thus the carrier recombination will not be facilitated.

Thus, to discuss the effects of the secondary phase on the solar cell performance, it is essential to determine whether

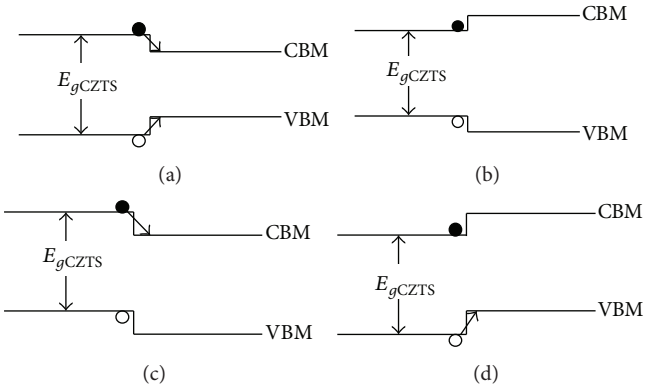

Figure 1: Band alignment of CZTS/secondary phase. (a) Type I heterointerface with E_g of the secondary phase smaller than that of CZTS. (b) Type I heterointerface with E_g of the secondary phase larger than that of CZTS. (c) Type II heterointerface with CBM and VBM in the secondary phase lower than that of CZTS. (d) Type II heterointerface with CBM and VBM in the secondary phase higher than that of CZTS.

the interface with the secondary phase is type I or II. However, the band alignment at the interface with the secondary phase has never been investigated either experimentally or theoretically so far. In this work, the influence ofsecondary phases of ZnS and CTS in CZTS absorber material is studied by calculating the band offsets at the CTS/CZTS/ZnS multilayer heterojunction interfaces on the basis of the first principles band structure calculation.

2. Calculation

The calculation of density of states (DOS) was performed on the basis of the first principles, density-functional, pseudopotential method using the PHASE code developed by Institute of Industrial Science, University Tokyo [20]. The valence electron configurations used in our calculations are S ($3s^2$, $3p^4$), Cu ($3d^{10}$, $4s^1$), Zn ($3d^{10}$, $4s^2$), and Sn ($4d^{10}$, $5s^2$, $5p^2$). We used the generalized gradient approximation (GGA) for the exchange-correlation interaction. For a given atomic arrangement, the lattice constants and atom positions were optimized to minimize the total energy.

2.1. Crystal Structure of Cu_2SnS_3. The most stable structure of CTS is reported to be the monoclinic structure with *Cc* symmetry [21], as shown in Figure 2. However, because of the lower symmetry, one cannot construct (monoclinic-CTS)/(kesterire-CZTS)/(zincblende-ZnS) supercell. CTS can also have a cubic or tetragonal structure, similar to the zincblende structure [21]. In this case, there is no difficulty due to symmetry mismatch in constructing a hetero supercell with CZTS and ZnS. However, in the zincblende-like structure of CTS, arrangement of Cu and Sn atoms is not perfectly ordered [21]. Since perfect periodicity of atom arrangement is needed for the band structure calculation, we consider the unit cells shown in Figure 3. The (001) layer of the metal sublattice alternately consists of (Cu, Sn), (Cu, Sn), and (Cu,Cu). The positions of Cu and Sn atoms are exchanged

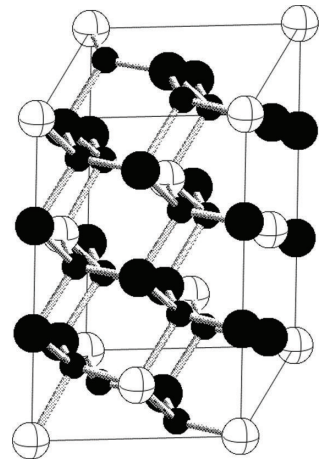

Figure 2: Monoclinic structure of Cu_2SnS_3.

or not exchanged between the two consecutive equivalent layers, and thus varieties of unit cells shown in Figure 3 can be considered.

First we calculated the lattice constant for these CTS structures, and the calculated lattice constants are the same for all; that is, $a = 0.55$ nm and $c = 1.644$ nm. On the other hand, the total energy is different, lowest for structure-2. If we take the total energy zero for structure-2, the total energies are 2.5 meV/atom and 1.1 meV/atom for structure-1 and structure-3, respectively. The energy difference is small, and considering limited accuracy of calculation, we could not definitively conclude which is the most stable structure.

2.2. Density of State. Figure 4 shows the calculated density of states (DOS) for (a) structure-2 (tetragonal structure) of CTS, (b) for zincblende ZnS, and (c) for kesterite CZTS. In DOS for both CTS and CZTS, the states near VBM are derived from interaction of S 3p and Cu 3d orbital, and the lowest conduction band is composed of S 3p and Sn 5s orbitals [21]. The reported value of band gap is 0.9 eV for CTS [21] and 3.7 eV for ZnS [22].

3. Results and Discussion

To evaluate the band offset, we consider a supercell consisting one unit cell of CTS, one unit cell of CZTS, and two unit cells of ZnS. For CTS, the (001) layer of the metal sublattice consists of (Cu, Sn) or (Cu, Cu). For kesterite CZTS, the (001) layer of the metal sublattice consists of (Cu, Sn) or (Cu, Zn). Thus, there are six different CTS/CZTS/ZnS supercells with different arrangements of the interface layer atoms as shown in Table 1. Interface 1 is between CTS and CZTS, interface 2 between CZTS and ZnS, and interface 3 between ZnS and CTS. The lattice constant parallel to the interface is assumed to be equal to that of the dominant material CZTS; that is, $a = 0.551$ nm. The lattice spacing in the perpendicular direction is assumed to be the same as in the respective bulk materials.

Table 1 lists the calculated valence band offsets and total energies for the six supercells with different arrangements of the interface layer atoms. The VBM energy averaged in

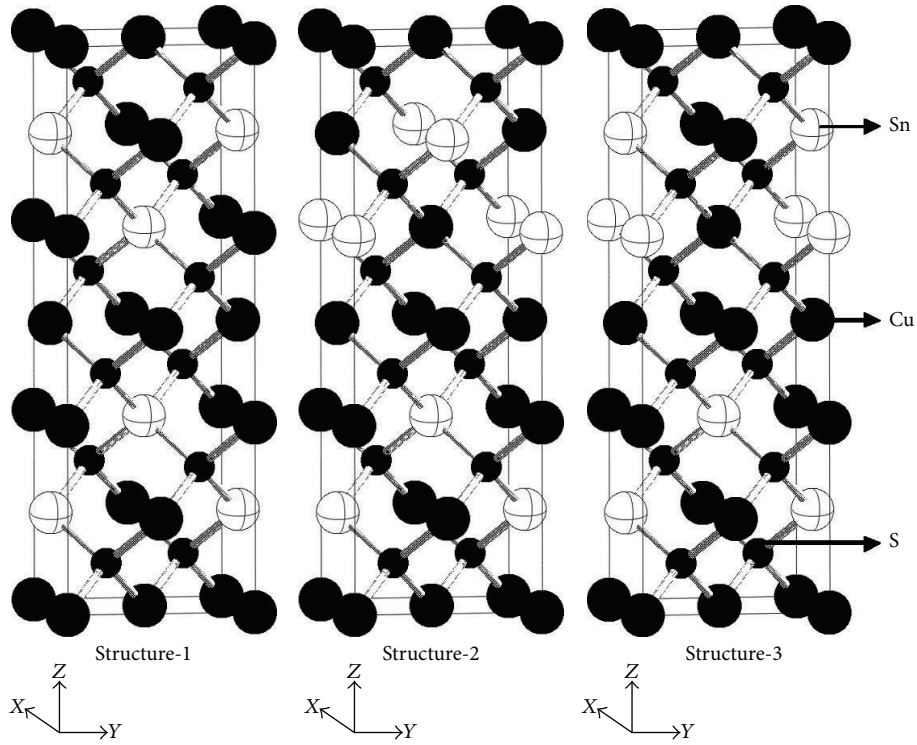

Figure 3: Unit cells for Cu_2SnS_3 with different position of Cu and Sn atoms in the (Cu, Sn) layers.

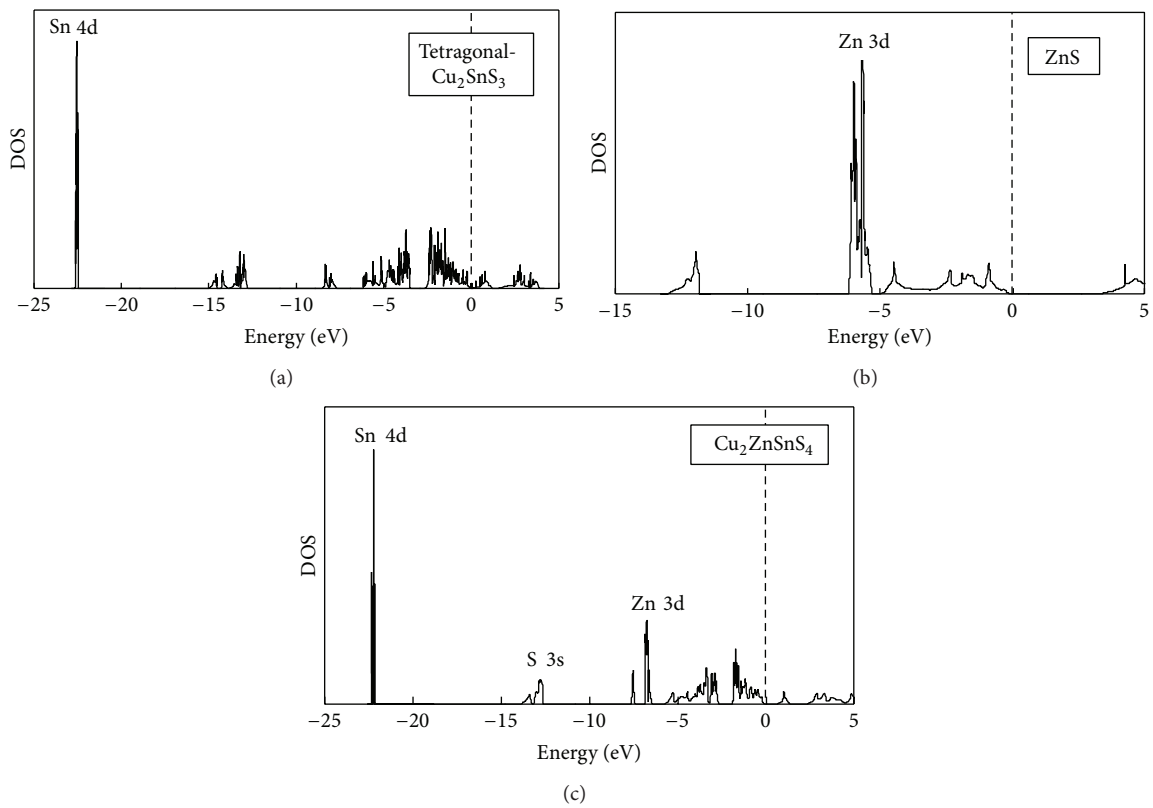

Figure 4: Density of states (a) for tetragonal structure of CTS, (b) for ZnS, and (c) for kesterite CZTS.

Table 1: Valence band offsets (eV) at each interface and the total energies (meV/atom) for six supercells with different interface layer atoms. The interface between CTS and CZTS is interface 1, interface between CZTS and ZnS is interface 2, and interface between ZnS and CTS is interface 3.

	CTS-CZTS Interface 1	CZTS-ZnS Interface 2	ZnS-CTS Interface 3	ΔE_{v1}	ΔE_{v2}	ΔE_{v3}	ΔE_{total}
(1)	(Sn, Cu)-(Zn, Cu)	(Sn, Cu)-(Zn, Zn)	(Zn, Zn)-(Cu, Cu)	0.5	0.3	0.8	14.4
(2)	(Sn, Cu)-(Sn, Cu)	(Zn, Cu)-(Zn, Zn)	(Zn, Zn)-(Cu, Cu)	−0.1	0.1	0	27.9
(3)	(Sn, Cu)-(Zn, Cu)	(Sn, Cu)-(Zn, Zn)	(Zn, Zn)-(Sn, Cu)	0.4	1.4	1.8	0
(4)	(Sn, Cu)-(Sn, Cu)	(Zn, Cu)-(Zn, Zn)	(Zn, Zn)-(Sn, Cu)	0.1	0.8	0.9	5.2
(5)	(Cu, Cu)-(Zn, Cu)	(Sn, Cu)-(Zn, Zn)	(Zn, Zn)-(Sn, Cu)	0	1.8	1.8	27.7
(6)	(Cu, Cu)-(Sn, Cu)	(Zn, Cu)-(Zn, Zn)	(Zn, Zn)-(Sn, Cu)	−0.2	0.8	0.6	13.2

each layer was used to calculate the band offset. ΔE_{v1} is the band offset at CTS/CZTS interface, and a positive value indicates that VBM of CTS is higher than that of CZTS. ΔE_{v2} is the band offset at CZTS/ZnS interface, and a positive value indicates that VBM of CZTS is higher than that of ZnS. ΔE_{v3} is the band offset at ZnS/CTS interface, and a positive value indicates that VBM of CTS is higher than that of ZnS.

The total energy per atom is given with the energy of supercell (3) taken as zero. From Table 1, one can see that the total energies are relatively small for supercells (3) and (4). In these cells, the average value of valence electrons is near two for the four adjacent metal atoms at all of the three interfaces, and thus the octet rule is almost fulfilled. In contrast, in supercell (5), the (Cu, Cu)-(Zn, Cu) interface has a high energy, and in supercell (2), both the (Sn, Cu)-(Sn, Cu) and (Zn, Zn)-(Cu, Cu) interfaces have a relatively high energy, because of violation of the octet rule.

Because the total energy is relatively lower for supercells (3) and (4) as listed in Table 1, the band alignment for supercell (3) and supercell (4) is shown in Figure 5. VBM of CZTS is below that of CTS (ΔE_v = 0.4 and 0.1 eV), and VBM of ZnS is below that of CZTS (ΔE_v = 1.4 and 0.8 eV). Considering that the band gaps are 3.7 eV for ZnS, 0.9 eV for CTS, and 1.5 eV for CZTS, CBM of CTS is below that of CZTS (ΔE_c = 0.2 and 0.5 eV), and CBM of CZTS is below that of ZnS (ΔE_c = 0.8 and 1.4 eV).

Barkhouse et al. measured the band offset at ZnS/$CuZnSn(S_{0.4}Se_{0.6})_4$ by laser pump/probe ultraviolet photoemission spectroscopy [23]. $Cu_2ZnSn(S_{0.4}Se_{0.6})_4$ has a band gap of 1.2 eV, smaller than that of CZTS by 0.3 eV, and the measured value of ΔE_v is 1.3 eV. The present results for ZnS/CZTS seem not inconsistent with their results.

Thus, the band alignment of ZnS/CZTS interface is of type I, and there is large spike (>0.8 eV) for both the conduction and valence bands. Such a large spike will create a high resistance barrier to carrier flows. Thus, the ZnS phase may hinder the flow of photo-excited carriers (electrons), reducing the photo current, and impede the flow of majority carriers (holes), increasing the series resistance [17, 23, 24]. On the other hand, since ZnS can expel both the carriers, the recombination rate in ZnS can be low. In addition, since the lattice constant of ZnS (0.541 nm) is close to that of CZTS (a = 0.551 nm), the interface will not have high density of defects. Therefore, if the surface or boundary of CZTS grains is covered with ZnS, recombination at the surface/boundary will be suppressed. In fact, Mendis et al. found that the ZnS/CZTS has a low recombination velocity [17].

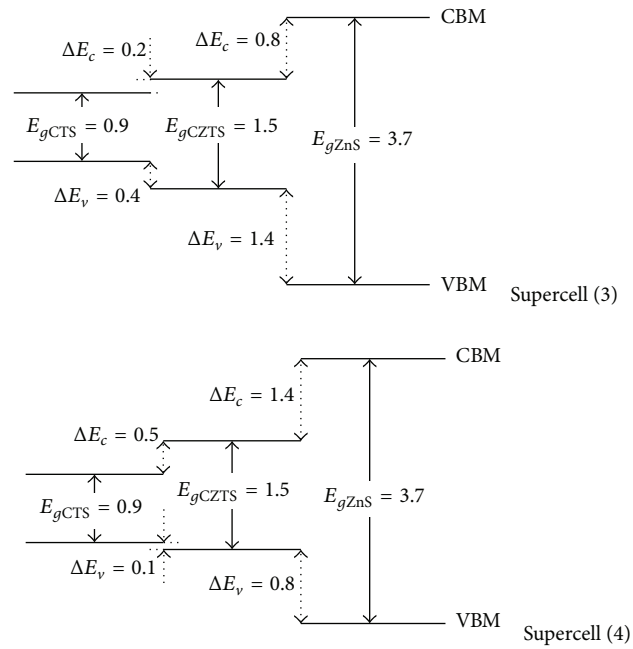

Figure 5: Predicted band alignments for supercell (3) and supercell (4) of CTS/CZTS/ZnS.

As shown in Figure 5, the band alignment of CTS/CZTS interface is also of type I. CTS can be regarded as a cluster of (Sn_{Zn} + $2Cu_{Zn}$) defect pairs in CZTS. The formation of (Sn_{Zn} + $2Cu_{Zn}$) defect pairs can shift VBM upward because the formation of Cu_{Zn} enhances the p-d repulsion and shift CBM downward because the formation of Sn_{Zn} makes CBM wavefunction more localized on the more electronegative Sn sites [18, 21]. Therefore, CBM and VBM of CTS are located within the forbidden energy region of CZTS. In this case, since CTS has a smaller band gap, both of minority and majority carriers will flow to CTS. Thus the CTS phase in CZTS will act as a recombination center, lowering both output current and voltage. If the CZTS surface is covered with CTS, CTS is expected to act as a sink for carriers and enhance the surface recombination velocity. However, according to Mendis et al., the CTS/CZTS interface also has a low recombination velocity [17]. Thus, their results cannot

be interpreted on the basis of the band alignment but could be related with other factors such as space charge distribution near the interface.

The present results show that the CTS phase is definitely detrimental for the solar cell performance. Thus, Zn-rich composition is preferable to prevent formation of CTS, although excessively Zn-rich composition will result in dominance of the highly resistive ZnS phase and reduce the solar cell efficiency.

In this work, we consider only the (001) interface. In fact, the band offset may depend on the interface orientation [15]. The actual CZTS layers in solar cells are polycrystalline, and thus the interface with the secondary phases can have various orientations. Therefore, for more accurate prediction of the band offset, the calculation had better be done for the other orientations. However, for the orientations other than (001), we need to consider a much larger supercell. For example, the supercell needed for the calculation of the (010) interface is six times larger than that for the (001) orientation. Since we cannot perform the calculation for such a large cell because of the limited computational power, we consider only the (001) orientation. In general, the band offset is expected to be determined by the two factors. One is the position of VBM with respect to an absolute reference level, and the other is the interface charge-dipole, which causes discontinuity in the electrostatic potential. The second one will depend on the interface orientation, but the first factor is common for any interface orientation. Thus, we may expect that the calculation for only one orientation is still useful to qualitatively predict the band offset.

4. Conclusions

In this study, we have calculated the band offsets at the CTS/CZTS/ZnS heterojunction interfaces on the basis of the first principles band structure calculation. The ZnS/CZTS heterointerface is of type I, and since ZnS has a larger band gap than that of CZTS, the ZnS phase in CZTS is predicted to be resistive barriers for carriers. The CTS/CZTS heterointerface is also of type I, and CBM and VBM of CTS are located within the band gap of CZTS. Therefore, the CTS phase will act as a recombination site in CZTS. It should be noted that comparison to experiment is limited by the limits of computing power and that there may be some discrepancies due to inability to carry out more generalized computational modeling.

Conflict of Interests

The authors declare that there is no conflict of interests regarding the publication of this paper.

Acknowledgment

The authors would like to thank Dr. M. Kato for his useful discussion.

References

[1] A. Ennaoui, M. Lux-Steiner, A. Weber et al., "Cu_2ZnSnS_4 thin film solar cells from electroplated precursors: novel low-cost perspective," *Thin Solid Films*, vol. 517, no. 7, pp. 2511–2514, 2009.

[2] H. Katagiri, K. Jimbo, S. Yamada et al., "Enhanced conversion efficiencies of Cu_2ZnSnS_4-based thin film solar cells by using preferential etching technique," *Applied Physics Express*, vol. 1, no. 4, Article ID 041201, 2008.

[3] N. Nakayama and K. Ito, "Sprayed films of stannite Cu_2ZnSnS_4," *Applied Surface Science*, vol. 92, pp. 171–175, 1996.

[4] K. Tanaka, M. Oonuki, N. Moritake, and H. Uchiki, "Cu_2ZnSnS_4 thin film solar cells prepared by non-vacuum processing," *Solar Energy Materials and Solar Cells*, vol. 93, no. 5, pp. 583–587, 2009.

[5] H. Wang, "Progress in thin film solar cells based on Cu_2ZnSnS_4," *International Journal of Photoenergy*, vol. 2011, Article ID 801292, 10 pages, 2011.

[6] A. Weber, H. Krauth, S. Perlt et al., "Multi-stage evaporation of Cu_2ZnSnS_4 thin films," *Thin Solid Films*, vol. 517, no. 7, pp. 2524–2526, 2009.

[7] H. Katagiri, "Cu_2ZnSnS_4 thin film solar cells," *Thin Solid Films*, vol. 480-481, pp. 426–432, 2005.

[8] K. Wang, O. Gunawan, T. Todorov et al., "Thermally evaporated Cu_2ZnSnS_4 solar cells," *Applied Physics Letters*, vol. 97, no. 14, Article ID 143508, 2010.

[9] B. Shin, O. Gunawan, Y. Zhu, N. A. Bojarczuk, S. J. Chey, and S. Guha, "Thin film solar cell with 8.4% power conversion efficiency using an earth-abundant Cu_2ZnSnS_4 absorber," *Progress in Photovoltaics*, vol. 21, no. 1, pp. 72–76, 2013.

[10] A. Redinger, K. Hönes, X. Fontań et al., "Detection of a ZnSe secondary phase in coevaporated $Cu_2ZnSnSe_4$ thin films," *Applied Physics Letters*, vol. 98, no. 10, Article ID 101907, 2011.

[11] M. Bär, B. A. Schubert, B. Marsen et al., "Impact of KCN etching on the chemical and electronic surface structure of Cu_2ZnSnS_4 thin-film solar cell absorbers," *Applied Physics Letters*, vol. 99, no. 15, Article ID 152111, 2011.

[12] K. Wang, B. Shin, K. B. Reuter, T. Todorov, D. B. Mitzi, and S. Guha, "Structural and elemental characterization of high efficiency Cu_2ZnSnS_4 solar cells," *Applied Physics Letters*, vol. 98, no. 5, Article ID 051912, 2011.

[13] C. Platzer-Björkman, J. Scragg, H. Flammersberger, T. Kubart, and M. Edoff, "Influence of precursor sulfur content on film formation and compositional changes in Cu_2ZnSnS_4 films and solar cells," *Solar Energy Materials and Solar Cells*, vol. 98, pp. 110–117, 2012.

[14] S. Chen, X. G. Gong, A. Walsh, and S. H. Wei, "Defect physics of the kesterite thin-film solar cell absorber Cu_2ZnSnS_4," *Applied Physics Letters*, vol. 96, no. 2, Article ID 021902, 2010.

[15] A. Nagoya, R. Asahi, R. Wahl, and G. Kresse, "Defect formation and phase stability of Cu_2ZnSnS_4 photovoltaic material," *Physical Review B*, vol. 81, no. 11, Article ID 113202, 2010.

[16] T. Kato, H. Hiroi, N. Sakai, S. Muraoka, and H. Sugimoto, "Characterization of front and back interfaces on Cu_2ZnSnS_4 thin-film solar cells," in *Proceedings of the 27th European Photovoltaic Solar Energy Conference and Exhibition*, 3CO.4.2, pp. 2236–2239, 2012.

[17] B. G. Mendis, M. C. J. Goodman, J. D. Major, A. A. Taylor, K. Durose, and D. P. Halliday, "The role of secondary phase precipitation on grain boundary electrical activity in Cu_2ZnSnS_4 (CZTS) photovoltaic absorber layer material," *Journal of Applied Physics*, vol. 112, no. 12, Article ID 124508, 2012.

[18] S. Chen, J. H. Yang, X. G. Gong, A. Walsh, and S.-H. Wei, "Intrinsic point defects and complexes in the quaternary kesterite semiconductor Cu_2ZnSnS_4," *Physical Review B*, vol. 81, no. 24, Article ID 245204, 2010.

[19] T. Gokmen, O. Gunawan, T. K. Todorov, and D. B. Mitzi, "Band tailing and efficiency limitation in kesterite solar cells," *Applied Physics Letters*, vol. 103, no. 10, Article ID 103506, 2013.

[20] http://www.ciss.iis.u-tokyo.ac.jp/rss21/en/.

[21] Y.-T. Zhai, S. Chen, J.-H. Yang et al., "Structural diversity and electronic properties of Cu_2SnX_3 (X=S, Se): a first-principles investigation," *Physical Review B*, vol. 84, no. 7, Article ID 075213, 2011.

[22] A. Ebina, E. Fukunaga, and T. Takahashi, "Reflectivity spectra of structurally pure wurtzite-type ZnS in ultraviolet and vacuum-ultraviolet regions," *Physical Review B*, vol. 12, no. 2, pp. 687–689, 1975.

[23] D. A. R. Barkhouse, R. Haight, N. Sakai, H. Hiroi, H. Sugimoto, and D. B. Mitzi, "Cd-free buffer layer materials on $Cu_2ZnSn(S_xSe_{1-x})_4$: band alignments with ZnO, ZnS, and In_2S_3," *Applied Physics Letters*, vol. 100, no. 19, Article ID 193904, 2012.

[24] J. Timo Wätjen, J. Engman, M. Edoff, and C. Platzer-Björkman, "Direct evidence of current blocking by ZnSe in $Cu_2ZnSnSe_4$ solar cells," *Applied Physics Letters*, vol. 100, no. 17, Article ID 173510, 2012.